Experimental Visualization of Ion Thruster Neutralization Phenomena

IEPC-2013-107

Presented at the 33rd International Electric Propulsion Conference,
The George Washington University • Washington, D.C. • USA
October 6 – 10, 2013

Futoshi Tanaka[1] and Yoshinori Nakayama[2]
National Defense Academy of Japan, Yokosuka, Kanagawa, 239-8686, Japan

Abstract: Understanding of neutralization phenomena is important to develop ion thrusters with more efficient and long durability. In this study, a two-dimensional visualized ion thruster with a miniature microwave neutralizer was carried out for the investigation of neutralization phenomena. The thruster can emit the bright sheet-shaped ion beams and the neutralizer current can be controlled by the supplied microwave power. Through the observation in the downstream region and the measurement of the currents and potential, it was confirmed that the insufficient neutralizer current caused the ion beam width increase, space potential increase in the downstream region, and the semicircular luminescence zone formation in the region. It seemed that these phenomena were brought about by the formation of virtual anode, that the three-grid system had a certain level of durability to the neutralizer failure, and that the two- or three dimensional evaluations were necessary for the understandings of the neutralization phenomena.

Nomenclature

I_{ac} = acceleration grid current
I_b = beam current
I_{cv} = shield cover current
I_d = discharger current
I_{de} = deceleration grid current
I_f = filament current
I_{gc} = grid cover current
I_{sc} = screen grid current
I_n = neutralizer current
I_w = wall current
L_s = spatial gap
L_v = virtual anode position
NR = neutralization current ratio
n_p = plasma number density
T_e = electron temperature
T_g = target plate
V_p = space potential
V_d = discharger voltag
V_{ac} = screen grid potentia
V_s = net acceleration voltage
V_{sc} = screen grid potential

[1] Graduate Student, Department of Aerospace Engineering, em51028@nda.ac.jp
[2] Associate Professor, Department of Aerospace Engineering, ynakayam@nda.ac.jp

V_{tg} = target plate potential
V_v = virtual anode potential
x = position
φ = potential

I. Introduction

Ion thruster has a discharge chamber for ion production, a grid system for ion acceleration, and a neutralizer for spacecraft potential regulation. Since highly efficient plasma production and ion acceleration have been achieved by great efforts of many researchers, at present, many ion thrusters are installed in various satellites and spacecrafts as attractive space propulsion systems. The ion thruster installation was associated with the first successful of the asteroid sample return probe "Hayabusa" mission. It is safely to say that the embarking days of the initial development are gone, and the maturation days are coming. The understanding of neutralization phenomena is necessary for the maturation. This is because it was reported that the neutralizer failure brought about the deterioration and/or malfunction of ion thruster propulsion systems[1-3]. However, the understandings and the investigations seem to be difficult because the phenomena are sensitive for the direct measurements.

As reported in our papers, the ion beam optics and weakly plasma in the downstream region can be observed with the two-dimensional visualized ion thruster developed in our previous works[4,5]. This visualized ion thruster can be performed with the two-grid system or the three-grid system. Moreover, the electron current emitted from the miniature microwave neutralizer in our previous works can be controlled by the supplied microwave power. Accordingly, we considered that non-contact measurements with the visualized ion thruster and the microwave neutralizer may be useful for the investigation[6]. The objectives in this study are (1) to observe the ion beams and plasma near the grid system, (2) to evaluate the neutralization phenomena, and (3) to discuss the difference between the two-grid system optics and the three-grid system optics.

II. Neutralization

Ion thruster emits ions from its grid system. If the ion thruster system does not emit electrons as many as the ions, the ion thruster charges negatively. The emitted ions decelerate and stagnate in the downstream region of the thruster. The stagnant ions increase the space potential due to its space charge. This increased potential is called as "virtual anode" because the positive space charge potential acts on the ions as a positive electrode, that is, an anode. Figure 1 depicts the virtual anode potential due to imperfect neutralization [7-12]. The V_s and L_s in this figure mean the potential gap and spatial gap between the screen-grid (Sc) and the acceleration-grid (Ac). As shown in this figure, neutralization condition influences the potential and location of the virtual anode (V_v, L_v). The relations between the position (x) and the potential (φ) are expressed in the following equations with a ratio of V_v to V_s:

$$L_v = \left(1 - \sqrt{1 - \frac{V_v}{V_s}}\right)^{\frac{1}{2}} \left(1 + 2\sqrt{1 - \frac{V_v}{V_s}}\right) L_s \tag{1}$$

$$\frac{x}{L_s} = \frac{L_v}{L_s} \pm \left(\sqrt{1 - \frac{\varphi}{V_s}} - \sqrt{1 - \frac{V_v}{V_s}}\right)^{\frac{1}{2}} \left(\sqrt{1 - \frac{\varphi}{V_s}} + 2\sqrt{1 - \frac{V_v}{V_s}}\right) \tag{2}$$

Although this is based on one-dimension ideal model, this consideration has been used for the understandings of neutralization phenomena.

III. Experimental Apparatus and Procedure

A. Visualized Ion Thruster

The modified visualized ion thruster (hereafter called VIT-2) is used in this study. This VIT-2 was designed by the reference to the original VIT and its performance. The shape of the VIT-2 is two-dimensional rectangular parallelepiped, and the size of VIT-2 is larger than that of VIT. The schematic of the VIT-2 is depicted in Fig.2. This thruster is composed of a pair of rectangle glass plates, pure iron yokes, SmCo permanent magnets, a rectangle stainless steel grid system, and a plastic chassis (housing).

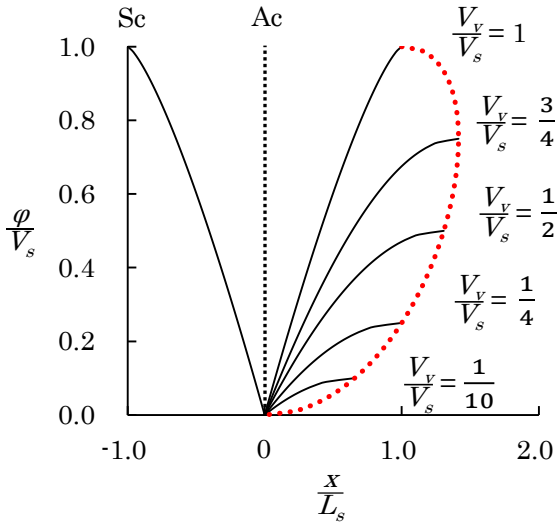

Fig.1. Virtual anode formation

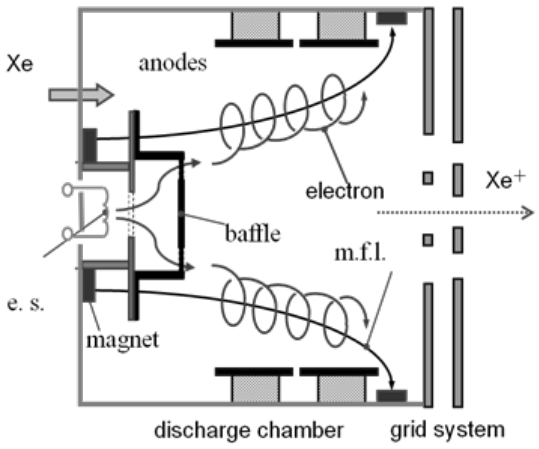

Fig.2. Schematic of VIT-2

The discharge chamber dimensions are 100 mm x 70 mm x 100 mm. The direct current discharge is produced in this thruster with a tungsten filament electron source, magnetic field and the potential difference between the anode and electron source. The typical number density (n_p) and electron temperature (T_e) near the grid system are 5.4×10^{16} m^{-3} and 3.0 eV, respectively. The typical space potential (V_p) is almost equal to the anode potential ($V_d + V_{sc}$). A stainless steel mesh surrounds the discharge chamber side-wall as a shield-cover for the prevention of neutralizer electron inflow.

The grid system is composed of a screen-grid (Sc), an acceleration-grid (Ac), deceleration-grid (De) and a pair of grid-covers (Gc). The dimensions and lengths are summarized in Table 1. A viewer can directly observe the ion beam optics because this slit grid system extract five sheet-shaped bright ion beams. More details are described in Refs. 4 and 5.

Table 1 Dimensions and lengths of grids

grid	material	voltage (V)	thickness (mm)	slit width (mm)	spatial gap (mm)
screen (Sc)	stainless steel	0～1500	1.0	6.0	2.0
accele (Ac)	stainless steel	-500	1.0	4.0	2.0
decele (De)	stainless steel	0	1.0	5.0	2.0

B. Miniature Microwave Neutralizer

The design of this neutralizer was based on that of the miniature microwave ion thruster: MINIT [13]. The neutralizer is composed of a cylindrical permanent magnet, a cylindrical yoke, a stainless steel microwave antenna and an orifice plate. The outer diameter of the magnet is 9.0 mm. Microwave power with a frequency of 2.45 GHz is supplied to the antenna via a DC-block. An aluminum-plate box with dimensions of 40 mm x 40 mm x 100 mm covers both the neutralizer body and the DC-block. This neutralizer is located at the downstream of the VIT-2, as shown in Fig.3.

In preliminary study, it was confirmed that the minimum operation flow rate and input power were 0.05 sccm (0.005 mg/s) and 0.1 W, respectively. This means that this neutralizer can be operated with low carrier gas flow and low luminescence intensity, and can little influence the neutralization phenomena. In addition, this neutralizer current can be controlled by the supplied microwave power

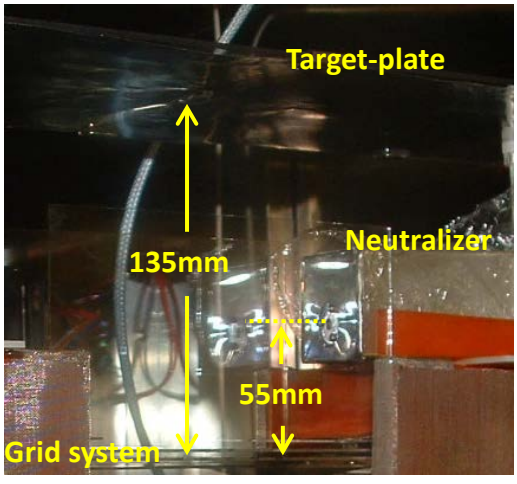

Fig.3. Miniature microwave neutralization

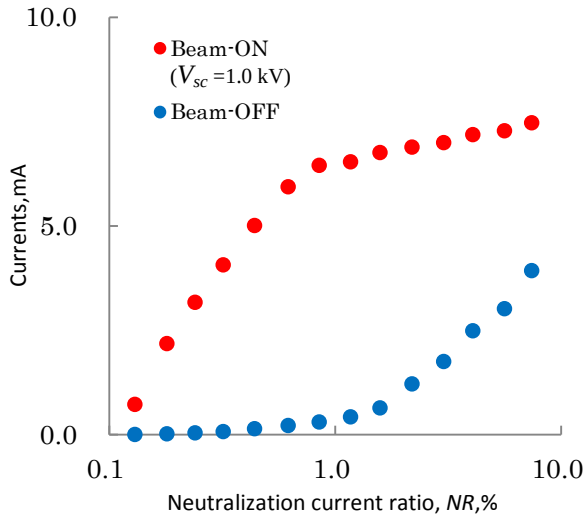

Fig.4. Neutralizer current

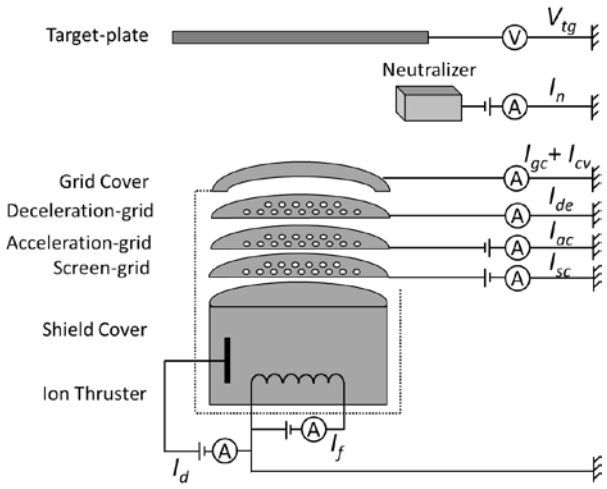

Fig.5. Schematic of the electric circuit

as shown in Fig.4. This means that the control of the supplied microwave power can intentionally set any neutralization condition. Judging from these performances, it seems that this neutralizer is appropriate for the evaluation of neutralization phenomena.

C. Experimental Procedure and Measurement

A schematic of the electric circuit for this study is indicated in Fig.5. The VIT-2 operates at the following conditions: xenon flow rate of 1.0 sccm (0.1 mg/s), discharge voltage (V_d) of 50 V, discharge current (I_d) of 0.30 A. The screen-grid potential (V_{sc}) is from 0.0 to 1.5 kV (0.1 kV step), and the acceleration-grid potential (V_{ac}) is -500 V. The neutralizer operates at a xenon flow rate of 0.1 sccm. The input microwave power of the neutralizer is from 0 to 7.4 W. A target-plate is located at 85 or 135 mm off the screen-grid. The ion beams and neutralization phenomena are imaged by a digital camera with a telecentric lens. The currents of the screen-grid (I_{sc}), acceleration-grid (I_{ac}), deceleration-grid (I_{de}), grid-cover (I_{gc}), shield-cover (I_{cv}), and the neutralizer (I_n) are measured individually with ammeters. The potential of target-plate (V_{tg}) is measured with a voltmeter. Since the internal resistance of the voltmeter is over 10 MΩ, the leak current is less than 0.1 mA that is equivalent to about 1% of the screen-grid current in case of 1.0 kV acceleration.

The minimum vacuum pressure is less than 0.1 mPa, and the typical vacuum pressure is less than 1.2 mPa during the operation of both the thruster and the neutralizer. In order to prevent the influence of the back pressure in the vacuum chamber to the neutralization phenomena, each experiment is carried out after over three-hour pumping with both a cryogenic pump and a turbo-molecular pump. The currents and the potential are measured against the screen-grid potential and/or the supplied microwave power. In this paper, the neutralization conditions are classified into the following cases: (1) “almost perfect neutralization case” (NR >95%), (2) “imperfect neutralization case” (5%< NR <95%), and (3) “little neutralization case” (NR <5%).

IV. Results and Discussion

D. Experimental Results and Accuracy

Before the discussion, the experimental results are summarized in this section. Figures 6 and 7 show the observed ion beams and the schematic current flows against the neutralization current ratio (NR) in the case of two-grid system and three-grid system, respectively. This neutralization current ratio (NR) is determined as the ratio of the neutralizer current (I_n) to the screen-grid current (I_{sc}) in this study. This ratio represents the level of interaction between the ions emitted from the ion source and the electrons emitted from the neutralizer. These results were obtained when the screen-grid (V_{sc}) potential was set at 1.0 kV. Figures 8a, 8b and 8c indicate the currents and the target-plate potential, against the neutralization current ratio (NR) in the case of two-grid system and three-grid system. Figure 8d indicates the target-plate potential (V_{tg}), against the screen-grid potential (V_{sc}) in the case of two-grid system and three-grid system. Figure 9 shows the observed ion beams when the target plate was located 85 and 135 mm off the screen-grid when the screen-grid potential (V_{sc}) was set at 0.5 kV in the case of two-grid system.

a) Almost perfect neutralization case, *NR* = 97%

b) Imperfect neutralization case, *NR* = 48%

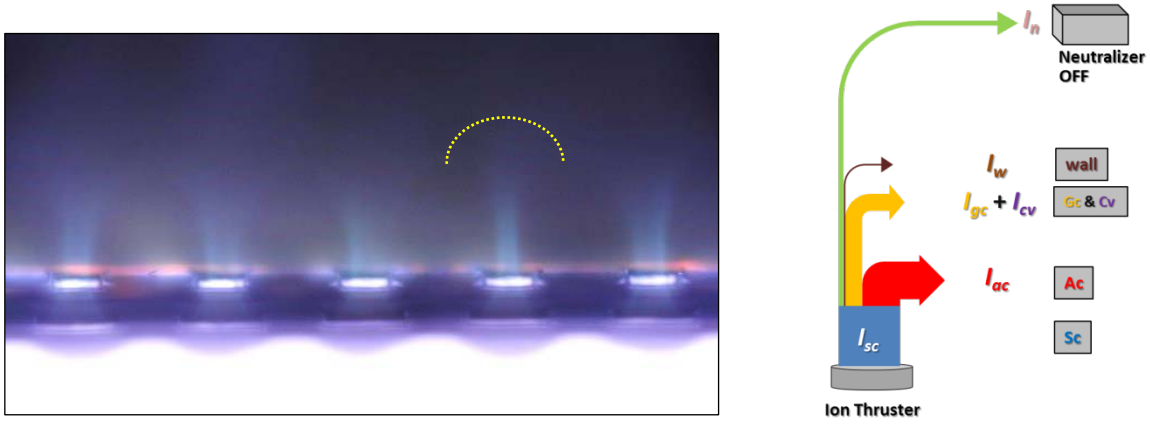

c) Little neutralization case, *NR* = 5%

Fig.6. Ion beam optics and schematic of current flows against neutralization current ratio (*NR*) (Two-grid system, V_{sc} =1.0kV) (Dashed lines indicate semicircular luminescence zones.)

a) Almost perfect neutralization case, NR = 99%

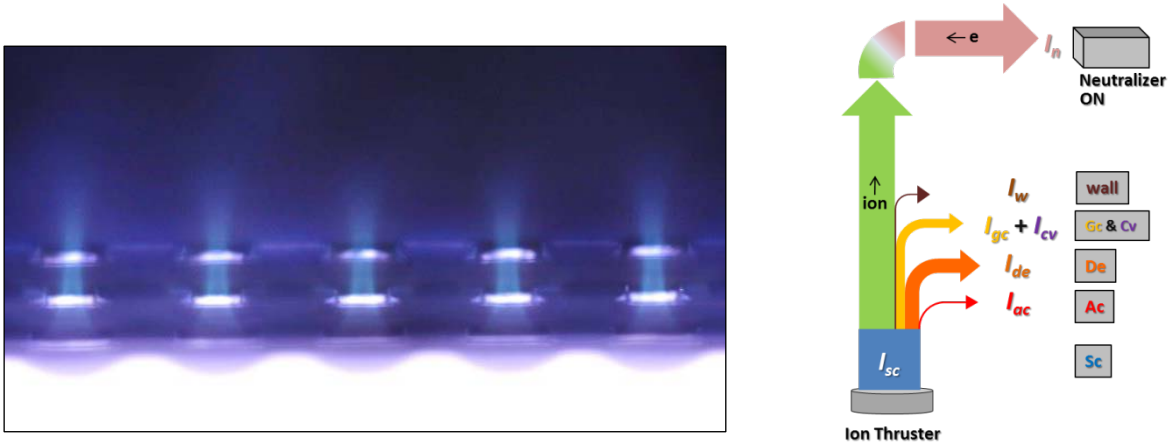

b) Imperfect neutralization case, NR = 50%

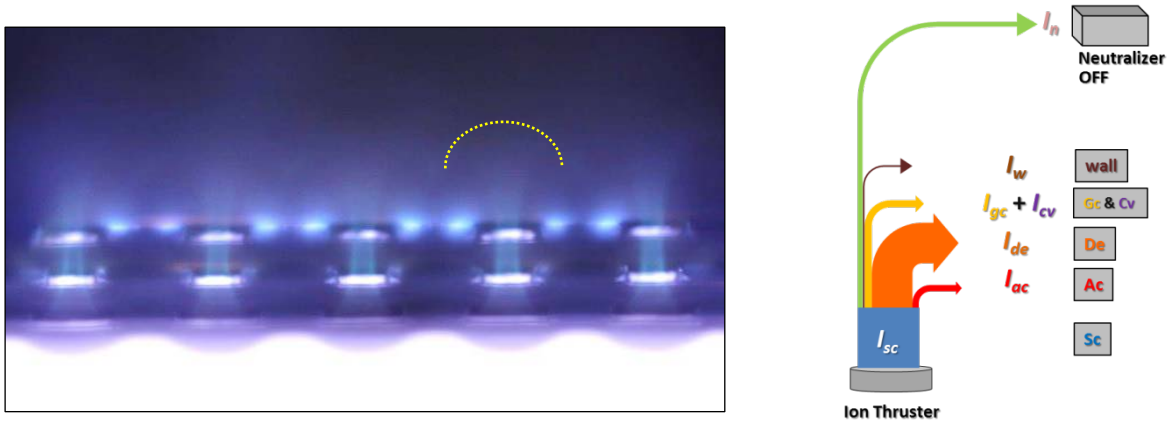

c) Little neutralization case, NR = 3%

Fig.7. Ion beam optics and schematic of current flows against neutralization current ratio (NR) (Three-grid system, V_{sc} =1.0kV) (Dashed lines indicate semicircular luminescence zones.)

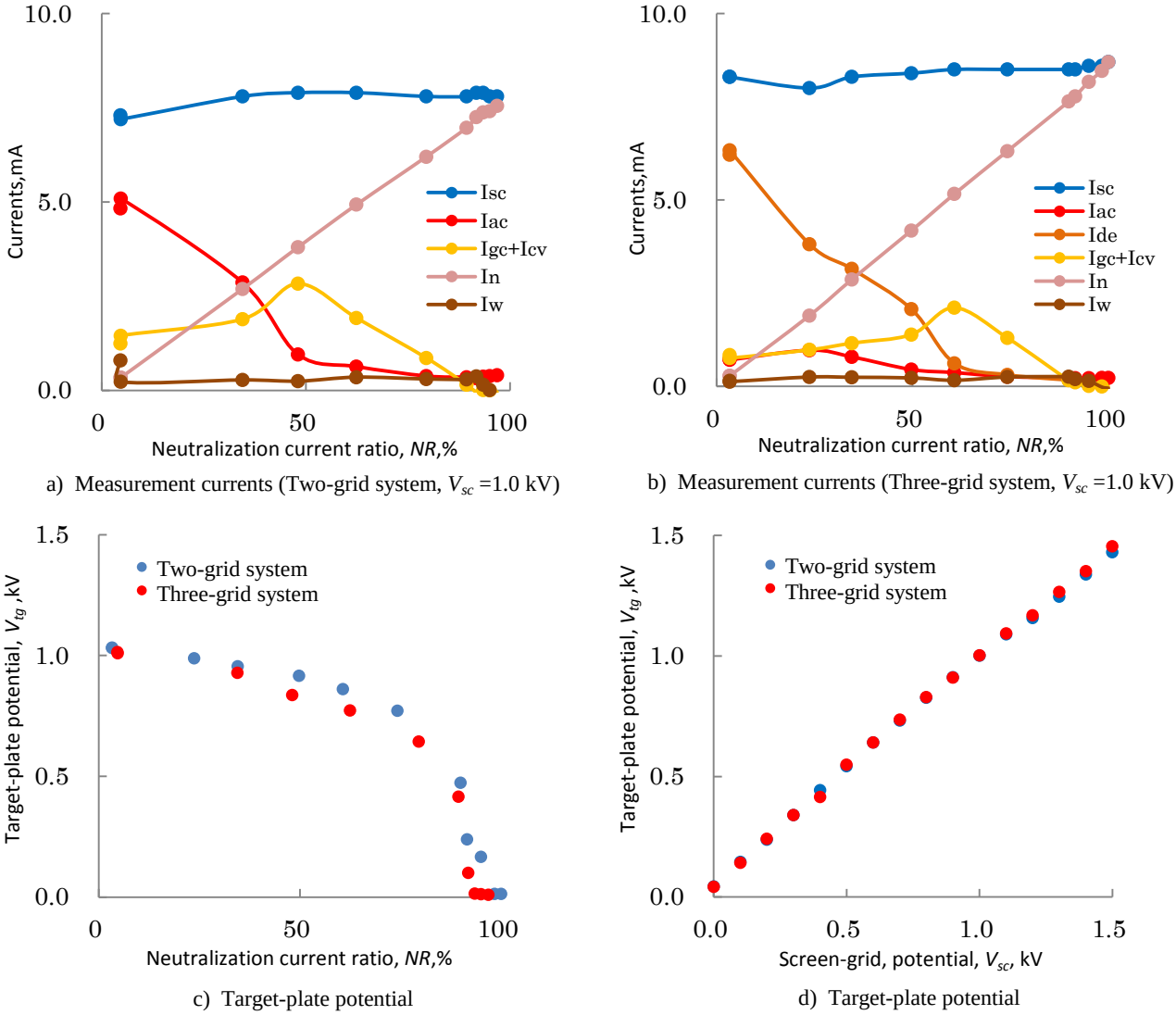

a) Measurement currents (Two-grid system, V_{sc} =1.0 kV)

b) Measurement currents (Three-grid system, V_{sc} =1.0 kV)

c) Target-plate potential

d) Target-plate potential

Fig.8. Measurement currents and target-plate potential

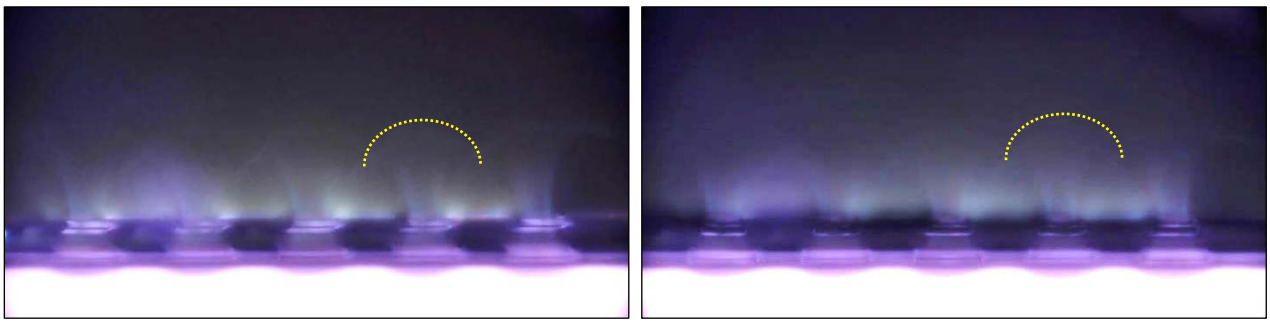

a) Target-plate location of 85 mm

b) Target-plate location of 135 mm

Fig.9. Ion beam optics (Two-grid system, Little neutralization case, V_{sc} = 0.5 kV)
(Dashed lines indicate semicircular luminescence zones.)

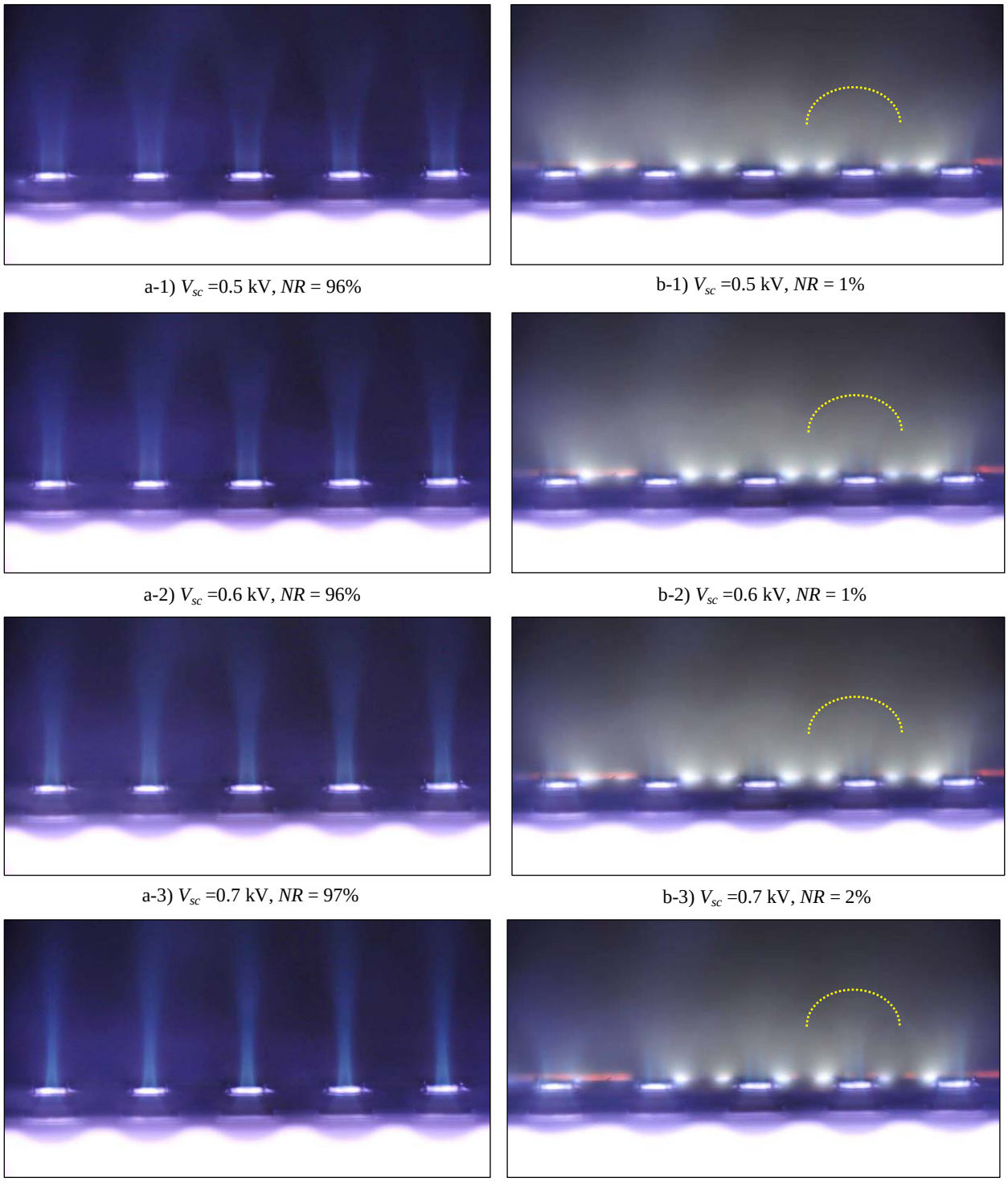

a-1) V_{sc} =0.5 kV, NR = 96%

b-1) V_{sc} =0.5 kV, NR = 1%

a-2) V_{sc} =0.6 kV, NR = 96%

b-2) V_{sc} =0.6 kV, NR = 1%

a-3) V_{sc} =0.7 kV, NR = 97%

b-3) V_{sc} =0.7 kV, NR = 2%

a-4) V_{sc} =0.8 kV, NR = 96%

b-4) V_{sc} =0.8 kV, NR = 3%

a) Almost neutralization case

b) Little neutralization case

Fig.10. Ion beam optics against screen-grid potential (V_{sc}) (Two-grid system)
(Dashed lines indicate semicircular luminescence zones.)

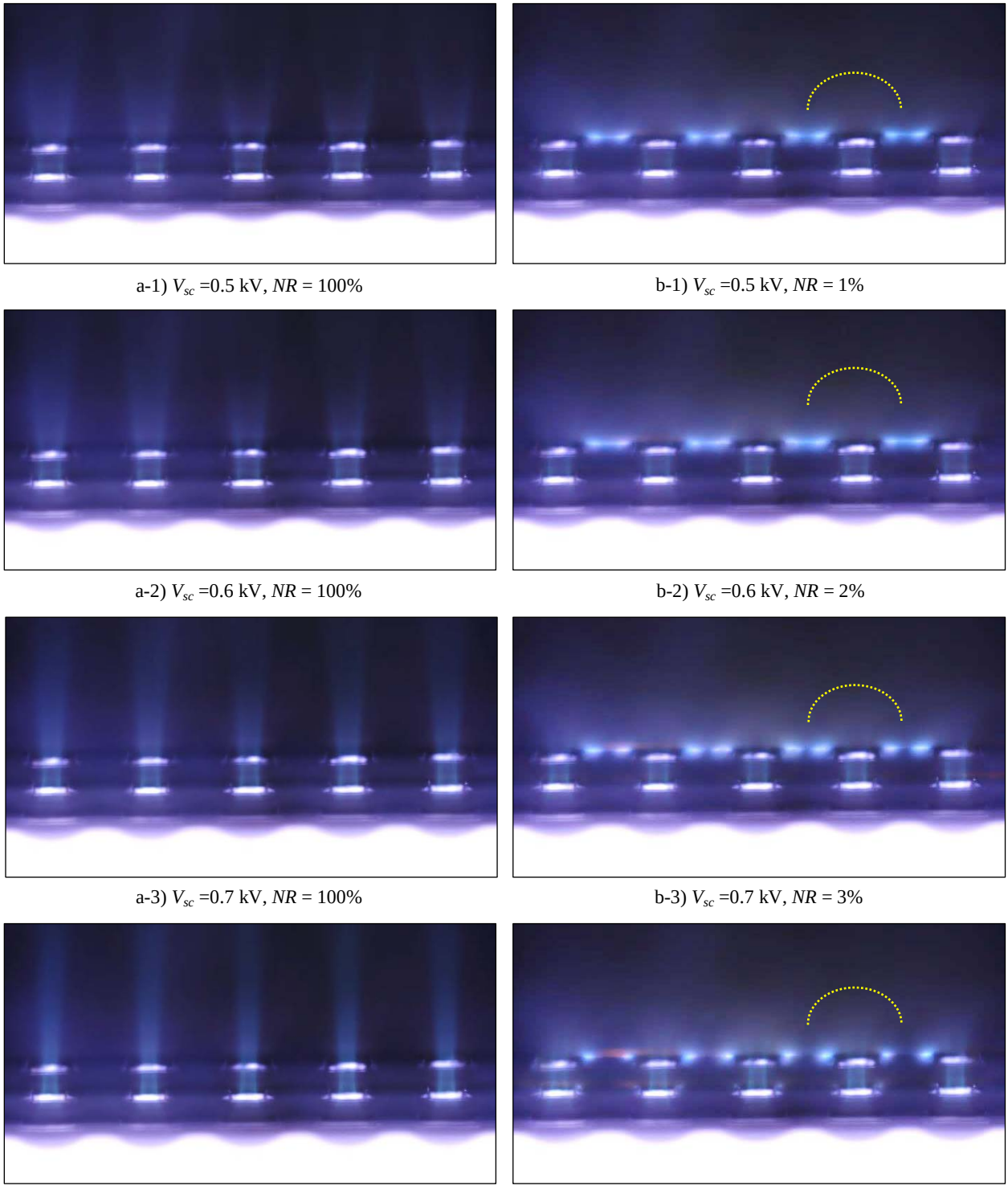

a-1) V_{sc} =0.5 kV, NR = 100%

b-1) V_{sc} =0.5 kV, NR = 1%

a-2) V_{sc} =0.6 kV, NR = 100%

b-2) V_{sc} =0.6 kV, NR = 2%

a-3) V_{sc} =0.7 kV, NR = 100%

b-3) V_{sc} =0.7 kV, NR = 3%

a-4) V_{sc} =0.8 kV, NR = 100%

b-4) V_{sc} =0.8 kV, NR = 4%

a) Almost neutralization case

b) Little neutralization case

Fig.11. Ion beam optics against screen-grid potential (V_{sc}) (Three-grid system)
(Dashed lines indicate semicircular luminescence zones.)

Figures 10 and 11 show the observed ion beams against the screen-grid potential (V_{sc}) in the case of two-grid system and three-grid system, respectively.

A. Ion Beam Optics

The followings are derived judging from Figs. 6, 7, 9, 10 and 11. :

1) In almost perfect neutralization case, the ion seems to flow almost linearly from the plasma sheath to the downstream region,
2) In the imperfect neutralization case, the emitted ion seems to be stagnant in the downstream region and to flow back to the acceleration grid and the beam width is wider than that in the almost perfect case,
3) In the little neutralization case, the stagnant phenomena (the semicircular luminescence zones), the backflow to grid system, and the beam width increase are clearly confirmed, and
4) The position of the semicircular luminescence zones is independent of the target position.

In addition, the following is also derived, judging from the difference of the grid system:

Little difference is confirmed. The position of the semicircular luminescence zones is the same in each system.

B. Current Flows and Target Plate Potential

The followings are derived judging from Figs. 8a, 8b, 8c and 8d :

1) In almost perfect neutralization case, the neutralizer current is equivalent to the beam current (I_b). The beam current is calculated by subtracting the acceleration-grid, grid-covers, shield cover and wall (I_w) currents from the screen grid current. The target-plate potential is almost zero,
2) In the imperfect neutralization case, the beam current is decreased and the currents of acceleration-grid and grid-covers and shield cover are increased. The increase is almost equivalent to the decrease. The target-plate potential increase with the decreasing neutralization current ratio (NR), and
3) In the little neutralization case, the beam current is almost zero, and the screen current is almost equivalent to the acceleration-grid, grid-covers and shield cover. The target-plate potential is almost equivalent to the screen-grid potential.

In addition, the following is also derived, judging from the difference of the grid system:

The acceleration-grid currents in the two-grid system case are almost equal to the deceleration-grid current(I_{de}) in the three-grid system case.

C. Evaluation of Neutralization Phenomena

Considering the above-mentioned, the followings are derived:

1) Since the target-plate is electrically isolated, the target-plate potential (V_{tg}) is almost equivalent to the spatial potential (φ) near the plate. Therefore, it seems that the increase of target-plate potential implies the numerous stagnant ions in the downstream region. Moreover, the semicircular luminescence zones were observed in the imperfect neutralization case, and the zones were clearly observed in the little neutralization case. Judging from these, it is likely that the zones are the virtual anodes [1,14],
2) Since the position and shape of the virtual anode is the same in each grid system, the formation of the virtual anodes is not dependent of the grid system, but of the neutralization condition (current ratio(NR)),
3) Since the stagnation of ions in the downstream region is supposed to increase the charge exchange phenomena, the imperfect neutralization deteriorates the durability of grid system,
4) Since the imperfect neutralization increases the acceleration-grid current in the two grid system case, the two-grid system has a vulnerability to the neutralizer failure,
5) Since the imperfect neutralization does not increase the acceleration-grid current in the three grid system case, the three-grid system has a certain level of durability to the neutralizer failure, as compared to the two-grid system,
6) Since the grid-cover current is detected in the imperfect neutralization cases, the position and shape of the grid-cover may influence the durability to the neutralizer failure, and
7) Since the observed luminescence zones are not one-dimensional in the imperfect neutralization cases, two- or three-dimensional model analysis is necessary to evaluate and understand of correct neutralization phenomena.

V. Conclusion

Through the observations and measurements of neutralization phenomena with a two-dimensional visualized ion thruster and a miniature microwave neutralizer, the followings were obtained:

1) The coupling use of both the visualized ion thruster and the miniature microwave neutralizer brought about the clearly observation of neutralization phenomena in the downstream of ion thruster grid system, due to the bright sheet-shaped ion beams of the thruster, low disturbance operation of the neutralizer,
2) Ion thruster can be normally operated with perfect neutralization,
3) Imperfect neutralization affected the ion beam optics in the downstream region, bought about formation of virtual anode, and reflux of ion flow to grid system. That is, imperfect neutralization deteriorates the durability of grid system, and
4) Neutralization was not one-dimensional phenomena. Two- or three-dimensional evaluations were necessary to understand the ion thruster neutralization phenomena.

References

[1] Kuninaka, H. and Molina-Morales, P., "Spacecraft charging due to lack of neutralization on ion thruster," *Acta Astoronautica*, Vol. 55., No. 1., 2004, pp.27-38.

[2] Nishiyama, K. and Kuninaka, H., "Discussion on Performance History and Operations of Hayabusa Ion Engines," *Transactions of JSASS Space Technology Japan*, Vol. 10, Pb.Tb_1-Tb_8, 2012.

[3] Ohmichi, W. and Kuninaka, H., "Degradation Mechanism of ECR Neutralizer and its Countermeasure," *32th International Electric Propulsion Conference*, IEPC-2011-314, Germany, 2011.

[4] Nakayama, Y., "Experimental Visualizationof Ion Thruster Discharge and Beam Extraction," *Transactions of JSASS Space Technology Japan*, Vol. 7, No. ists26, Pb_26-Pb_34, 2009.

[5] Nakayama, Y. and Teraura, Y., "Feasibility Study on Visualized Ion thruster," *30th International Electric Propulsion Conference*, IEPC-2007-043, Italy, 2007.

[6] Nakayama, Y., and Tanaka, F., "Experimental Evaluation of Neutralization Phenomena with Visualized Ion Thruster," *29th International Symposium on Space Technology and Science*, 2013-b-08, Japan, 2013

[7] Riege. H,. "Neutralization principles for the extraction and transport of ion beams," *Acta Astoronautica*, Vol. 451., No. 2., 2000, pp.394-405.

[8] Patterson, M. and Mohajeri, K., "NEUTRALIZER OPTIMIZATION," *22th International Electric Propulsion Conference*, IEPC-1991-151, Italy, 1991.

[9] Arakawa, Y. Kuninaka, H. Nakayama, Y. and Nishiyama, K., *Ion Engine for Powered Flight in Space*, Corona, Tokyo, 2006 (in Japanese).

[10] Jahn, R. G., *Physics of Electric Propulsion*, 1st ed., McGraw-Hill, New York, 1968, Chap. 7.

[11] Stuhlinger, E., *Ion Propulsion for Space Flight*, McGraw-Hill, New York, 1964.

[12] Lieberman, M. A., *Principle of Plasma Discharges and Materials Processing*, John Wiley & Sons, New York, 1994, pp154-159.

[13] Nakayama, Y., Funaki, I., Kuninaka, H. "Milli-Newton Class Miniature Microwave Ion Thruster," *Journal of Propulsion and Power*, Vol. 23., No. 2. ,2007, pp.495-499.

[14] Kuninaka, H., Funaki, I,. Nishiyama, K., Molina-Morales, P. and Nakayama Y., "Virtual Anode Phenomena Due to Lack of Neutralization on Ion Thusters Based on MUSES-C Program," *37th AIAA Joint Propulsion Conference*, AIAA-2001-3785, USA, 2001.